

# Wide-band slow light in compact photonic crystal coupled-cavity waveguides: supplementary material

MOMCHIL MINKOV\* AND VINCENZO SAVONA

Laboratory of Theoretical Physics of Nanosystems, Ecole Polytechnique Fédérale de Lausanne (EPFL), CH-1015 Lausanne, Switzerland

\*Corresponding author: momchil.minkov@epfl.ch

Published 1 July 2015

This document provides supplementary information to “Wide-band slow light in compact photonic crystal coupled-cavity waveguides,” <http://dx.doi.org/10.1364/optica.2.000631>. We outline the way the tight-binding model used in the paper is solved. A table summarizing the parameters for all designs is presented. Finally, the effect of small variations in the optimized parameters is studied, and no degradation of the important figures of merit is observed. © 2015 Optical Society of America

<http://dx.doi.org/10.1364/optica.2.000631.s001>

We present below the mathematics involved in obtaining the bands shown in Fig. 1(b) within a tight-binding model for a chain of cavities. We use the operator formalism that is standard in quantum mechanics, since it is concise and intuitive to read out, but we note that we are not discussing any quantum effects – the formalism is equally well suited to classical field propagation. We denote with  $c_i$  and  $c_i^\dagger$  the ladder operators for cavity  $i$ , with  $L_i$  the position of cavity  $i$ , and with  $L_y$  – the inter-cavity spacing. With first- and second-neighbor coupling and one cavity per unit cell, the Hamiltonian reads

$$H = \sum_i \left[ \frac{\omega_0}{2} c_i^\dagger c_i - t_1 (c_i^\dagger c_{i+1}) - t_2 c_i^\dagger c_{i+2} \right] + h.c. \quad (\text{S1})$$

Fourier transforming to  $k$ -space through  $c_j = \sum_k e^{ikL_j} c_k$ , this becomes

$$H(k) = \omega_0 - 2t_1 \cos(L_y k) - 2t_2 \cos(2L_y k), \quad (\text{S2})$$

and so the dispersion  $\omega(k)$  is given by

$$\omega(k) - \omega_0 = -2t_1 \cos(L_y k) - 2t_2 \cos(2L_y k), \quad (\text{S3})$$

where the Brillouin zone for  $k$  is from  $-\pi/L_y$  to  $\pi/L_y$ . If we consider instead the same system but written in terms of two cavities  $A$  and  $B$  in the unit cell, the Hamiltonian reads

$$H = \sum_i \left[ \frac{\omega_0}{2} (c_{Ai}^\dagger c_{Ai} + c_{Bi}^\dagger c_{Bi}) - t_1 (c_{Ai}^\dagger c_{Bi} + c_{Bi}^\dagger c_{Ai+1}) - t_2 (c_{Ai}^\dagger c_{Ai+1} + c_{Bi}^\dagger c_{Bi+1}) \right] + h.c. \quad (\text{S4})$$

Defining  $C_k = (c_{Ak}, c_{Bk})^T$ , the Fourier space Hamiltonian is  $H(k) = C_k^\dagger \mathcal{H}(k) C_k$ , with

$$\mathcal{H}(k) = \begin{pmatrix} \omega_0 - 2t_2 \cos(2L_y k) & -t_1(1 + e^{i2L_y k}) \\ -t_1(1 + e^{-i2L_y k}) & \omega_0 - 2t_2 \cos(2L_y k) \end{pmatrix} \quad (\text{S5})$$

Diagonalizing this 2-by-2 matrix gives the dispersion, which now consists of two bands but the Brillouin zone is twice smaller:  $k$  from  $-\pi/(2L_y)$  to  $\pi/(2L_y)$ . Since the system is physically the same, when ‘unfolded’, the two bands match the band obtained in eq. (S3). For a system with two cavities only, as in Fig. 2, the matrix for diagonalization to find the eigenmodes reads

$$\begin{pmatrix} \omega - \omega_0 & -t \\ -t & \omega - \omega_0 \end{pmatrix}, \quad (\text{S6})$$

and so  $\omega - \omega_0 = \pm t$ , from where we infer  $\Delta\omega = 2t$ .

**Table S1. Parameters and figures of merit of the optimized CCW designs presented in the main text.**

	Des. 1	Des. 2	Des. 3	Des. 4
$\Delta r_1/a$	-0.0385	-0.0049	-0.0221	0.0323
$\Delta r_2/a$	-0.0279	-0.0340	-0.0341	-0.0002
$\Delta r_3/a$	-0.0759	-0.1016	-0.1200	-0.0877
$\Delta x/a$	0.1642	0.2204	0.2500	0.2131
GBP	0.47	0.66	0.56	0.43
$\langle n_g \rangle$	37	116	88	51
$\Delta\lambda, [nm]$	19.5	8.8	9.9	13.1

In table S1 we summarize all the parameters and the relevant figures of merit of the four designs. The numbering follows the way the designs are presented in the main text: Des. 1 – Fig. 3; Des. 2 – Fig. 4(a)-(c); Des. 3 – Fig. 4(d)-(f); Des. 4 – Fig. 4(h)-(j).

The parameters are given with a high precision in case it is needed, but a sub-nanometer control is by no means a requirement to keep the outstanding dispersion properties. This is illustrated in Figs. S1 to S4, where we plot the effect of small variations of the optimization parameters on the wavelength dependence of the group index. In all figures, panel (a) shows variation in  $\Delta r_1$ , panel (b) – in  $\Delta r_2$ , panel (c) – in  $\Delta r_3$ , and panel (d) – in  $\Delta x$ . The red dashed line shows a variation of  $-2\text{nm}$  of the respective parameter, while the blue dashed line – of  $+2\text{nm}$ . This variation is larger than the state-of-the-art precision in Silicon devices. We note that  $\Delta r_1$  and  $\Delta r_2$  have a much more pronounced effect than  $\Delta r_3$  and  $\Delta x$ , which can be expected since the latter were introduced mostly to minimize losses. Most importantly, the effect of all parameters is to slightly shift the operational band up or down in wavelength, but the important property of the designs – high, approximately constant  $\langle n_g \rangle$  – is conserved.

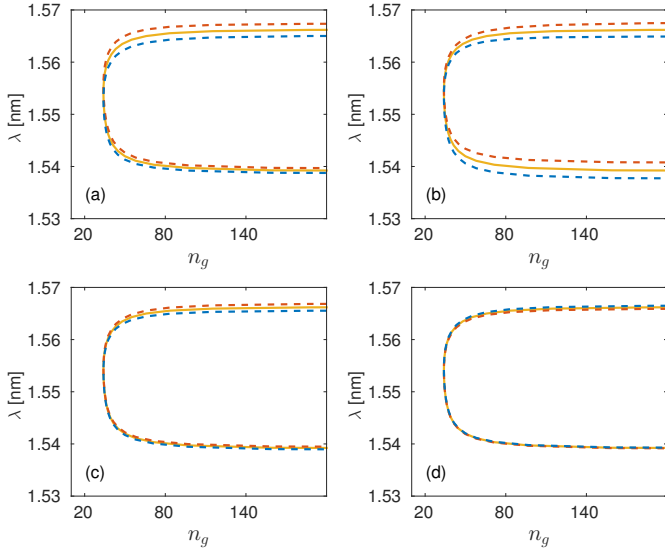


**Fig. S1.** Group index vs. wavelength for Design 1. Shown is the nominal structure (yellow solid line), and a  $-2\text{nm}$  (red dashed line) or a  $+2\text{nm}$  (blue dashed line) deviation in (a):  $\Delta r_1$ , (b):  $\Delta r_2$ , (c):  $\Delta r_3$ , and (d):  $\Delta x$ .

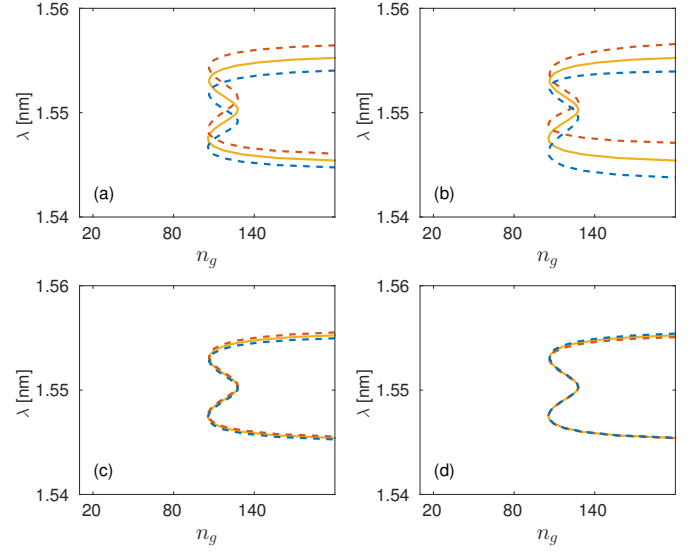


**Fig. S2.** Same as Fig. S1 but for Design 2.

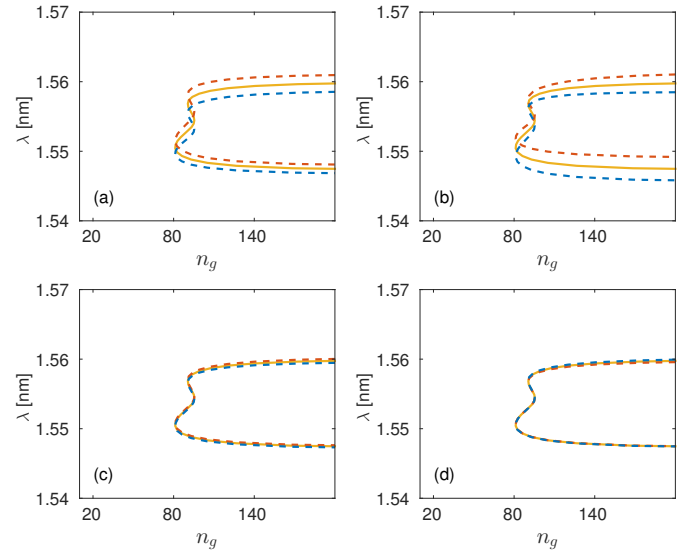


**Fig. S3.** Same as Fig. S1 but for Design 3.

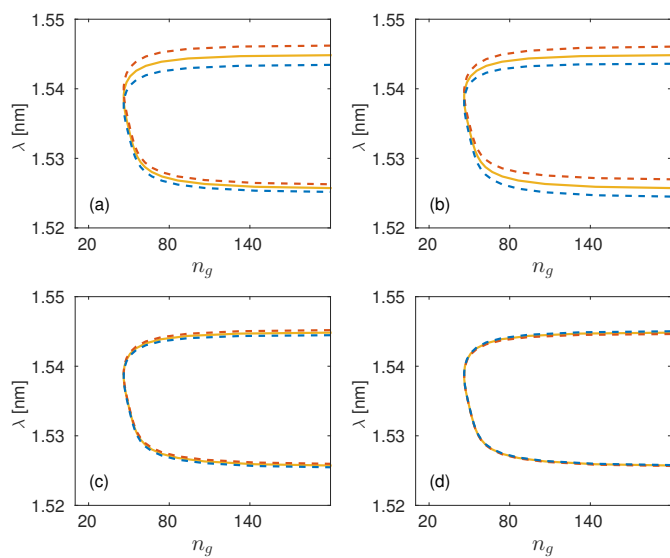


**Fig. S4.** Same as Fig. S1 but for Design 4.